Figure S1. Workflow of the ATAC-seq data collection, computational analysis, and experimental validation. ATAC-seq, Assay for Transposase-Accessible Chromatin with sequencing; FOX, forkhead box; PRAD, prostate adenocarcinoma; si, small interfering; TCGA, The Cancer Genome Atlas.

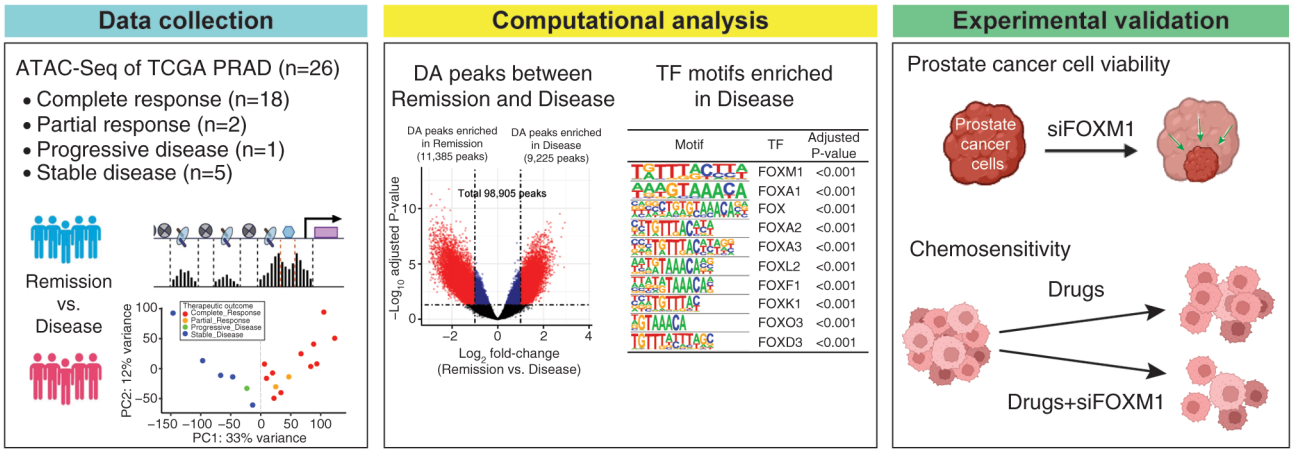

Figure S2. Differences in chromatin accessibility between the Remission and Disease groups. (A) Principal component analysis plot of the Assay for Transposase-Accessible Chromatin with sequencingsignal. (B) Hierarchical clustering of 26 patient samples.

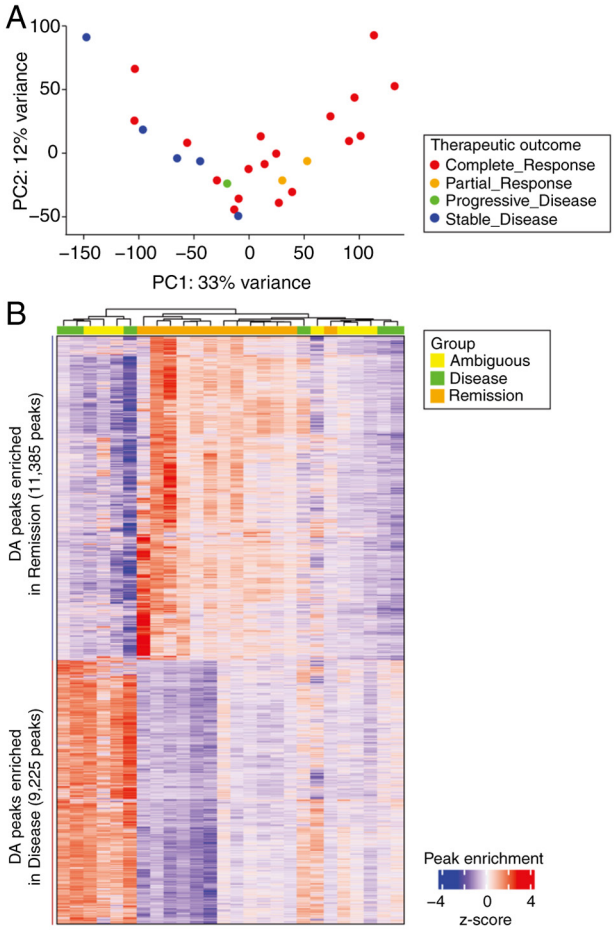

Figure S3. TF activities associated with the Remission and Disease groups. (A) Heatmap for TF activities. TFs significantly associated with the Remission group (34 TFs in blue) and Disease group (20 TFs in red) were identified based on an absolute mean TF activity difference >0.05 and the false discovery rateq-value=0.05. (B) Pearson correlation for 54 TF activities between the Remission and Disease groups. TF, transcription factor.

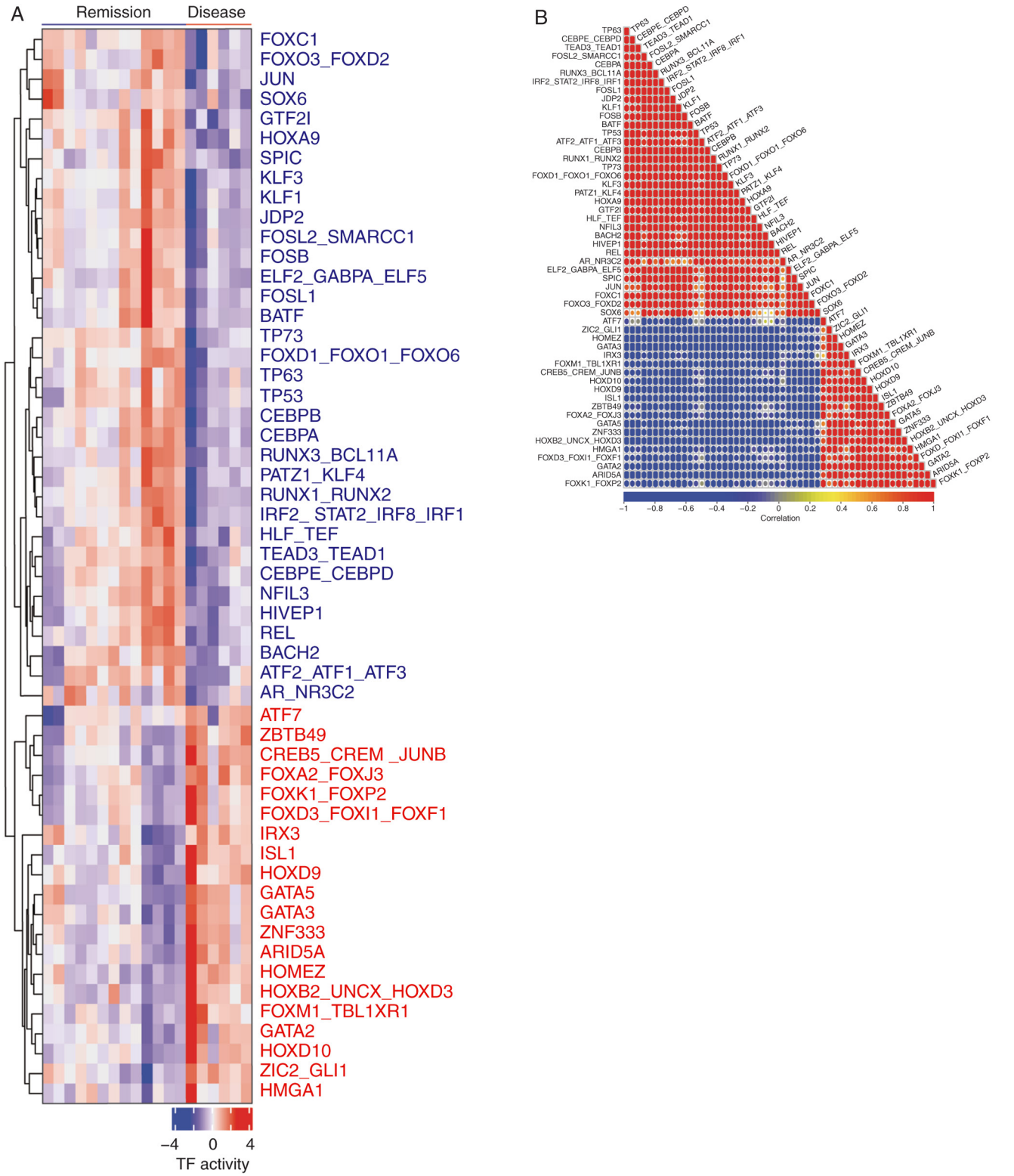

Figure S4. Representative images from the colony formation assay. FOX, forkhead box; si, small interfering.

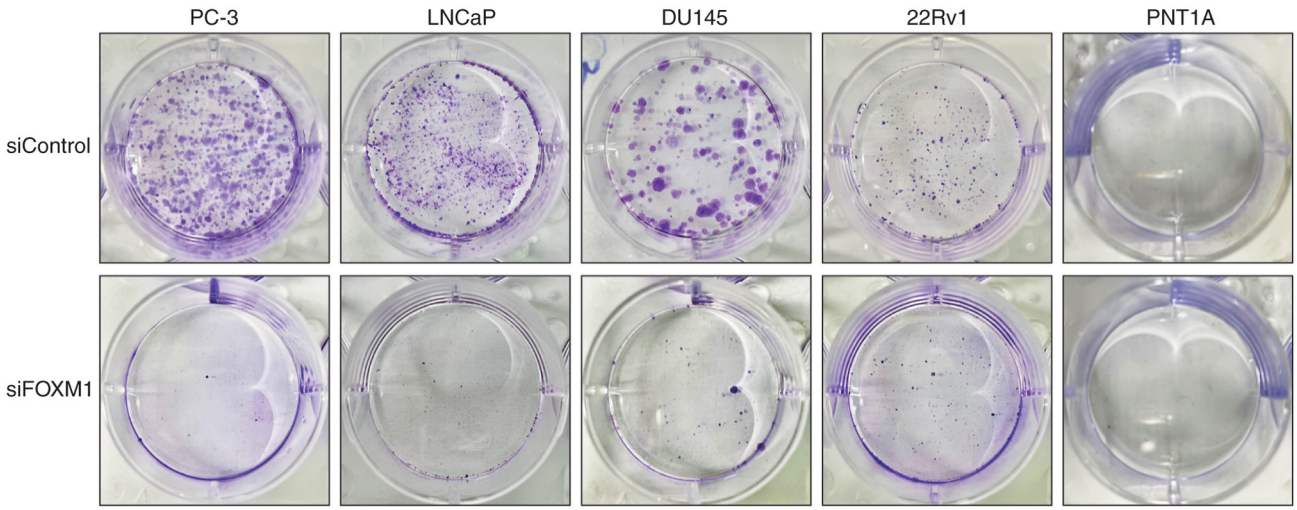

Figure S5. Effect of siFOXM1 on caspase-3 activation in prostate cancer cells. The ratio of cleaved caspase-3 to caspase-3 was plotted based on semi-quantification of the band intensities. Data are presented as the mean ± SEM (n=3). **P<0.01, ***P<0.005. FOX, forkhead box; n.s., not significant; si, small interfering.

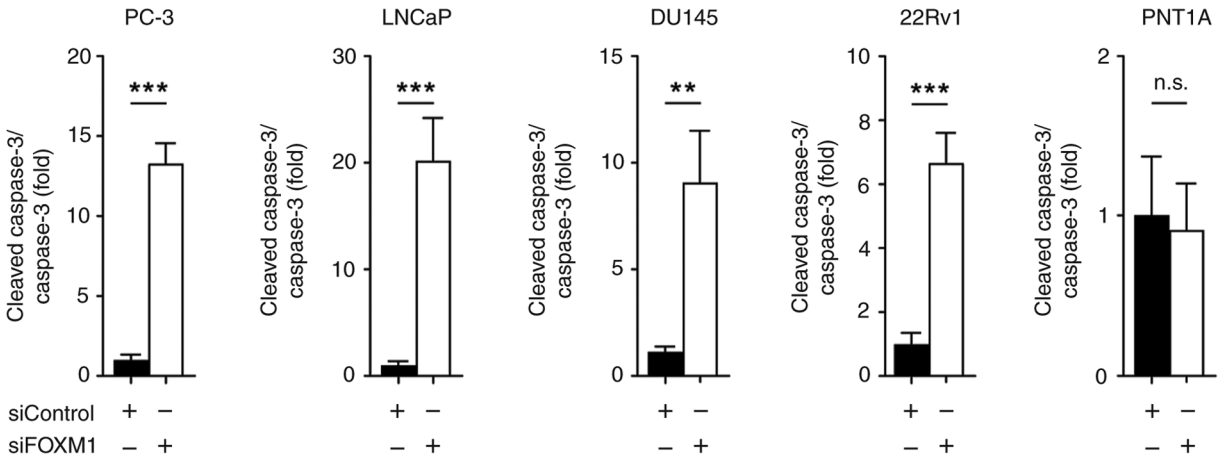

Figure S6. Co-expressional correlation plot between FOXM1 and AR in The Cancer Genome Atlas-prostate adenocarcinoma data. AR, androgen receptor; FOX, forkhead box.